



(٣٣٣) - (٣٥٣)

العدد الثاني
والعشرون

الحساب العددي لتأثير المجال المغناطيسي المائل على تعليق التدفق التمعجي المماس الزائدي في

وسط مسامي

زينب علي جعفر

قسم الفيزياء كلية التربية/ طوزخورماتو/ جامعة تكريت

zainabali611@tu.edu.iq

هنا ابراهيم لفتة

قسم الرياضيات/ مديرية تربية ديالى

hanaibra2022@gmail.com

المستخلص:

هدف البحث هو التحقيق في الحسابات العددية لتأثيرات المجال المغناطيسي المائل على النقل التمعجي لمائع المماس الزائدي اللانوتوني في وسط مسامي وقناه جيبيية غير متماثلة. تم العمل بتطبيق طريقه الاضطراب المنتظم العددية مع فرضيات عدد رينولدز المنخفض وطول الموجه الطويلة لغرض حل المعادلات التأسيسية غير الخطية في بعدين وبالصورة الكارتيزيه , الاستمرارية والحركة والطاقة بالإضافة الى معادلة التركيز. لعدد ويسنبرغ الصغير وجد الحل لكل من داله الجريان وتوزيع الحرارة, اضافه الى معادله التركيز وتم حسابها ومناقشه النتائج ورسومها بيانيا باستخدام البرنامج الرياضي ماتيماتكا.

الكلمات المفتاحية: المماس الزائدي، المجال المغناطيسي المائل، الوسط المسامي، التركيز، رقم فايسنبرغ.

Numerical computation for effect of inclined magnetic field on hyperbolic tangent peristalsis flow suspension in a porous medium.

Zainab A. Jaafar

Department of Physics, College of Education /Tuz Khurmatu, Tikrit

University, Tikrit, Iraq

zainabali611@tu.edu.iq

Hana I. Lafta



Department of Mathematic, Diyala Education Directorate, Diyala, Iraq
hanaibra2022@gmail.com

Abstract:

The desired goal of that research is to investigate the numerical calculations of the impacts of the inclined magnetic field a cross the peristalsis influx of non-Newtonian hyperbolic tangent fluid at a porous medium and an asymmetric sinusoidal channel. The work was done by applying the numerical uniform perturbation method with assumptions based on the length of the longitudinal wave and adding to the small Reynolds number for the purpose of solving non-linear constitutive equations in two dimensions and in the Cartesian form of continuity, motion and energy. In addition to the concentration equations, for small Wiesenberg number, the solution was found for both the stream function and the temperature distribution as well as the concentration equation. They were discussed and a graphic using the mathematical program "Mathematica" soft wire.

Keywords: Hyperbolic tangent, Inclined magnetic field, Porous Medium, Concentration, Weissenberg number.

1. Introduction

The study of PDEs incepted that in the 18th century AD. With a squad of scientists like Euler, Dalember and Lagrange, which appears in problem regarded to Sound, Energy, Fluid influx, elasticity and others. As a result of the importance of the magnificent role played by PDEs and to realize the solution of numerous of the mathematical physical, while engineering problems in an advanced mathematical mode, it was vital to found easier and further comprehensive methods for finding their solutions. PDEs are used in numerous phenomena in diverse Sciences and engineering and the target convey something from the PDEs and use them in applications. The rapid development in diverse types of sciences led to the wide spread use of mathematics, especially in Applied Sciences and this led to differential equations starting to play substantial role in those science. This was the beginning of the use of differential equations in natural sciences, because the laws of physics and chemistry are generally linked to a limited number of



known variables with the passage of time, the field of the use of differential equations expanded to include other science such as biomedical engineering, economics and engineering in its various branches. Every linear PDEs consists of one of the following types: parabolic, hyperbolic and elliptic equation. That is parabolic equations depict heat flow and diffusion processes and the following formula is fulfill $B^2 - 4Ac = 0$, the equations of the hyperbola are half of the vibrating movements, the wave movements and the following formula is fulfill $B^2 - 4Ac > 0$, the ellipse equations describe steady state phenomena and fulfill the following formula $B^2 - 4Ac < 0$ (Evans, 2022). The concept of peristalsis flow was developed for industrial objectives such as salutary fluid transfer, blood pump within heart lungs device and transfer of corrosive liquids when the osculate of the fluids for the machinery are forbidden. With all these contributions, a few theoretical with experimental studies have been done next the Seminal feet we cite them as an example (Hage & Hummady, 2022; Mekheimer, 2008; Nadeem et al., 2013). In some private cases of non-Newtonian fluids, a number of neoteric studies on peristalsis transfer of MHD have been achieved (Hayat, Rafiq, et al., 2016; Kumar, 2016; Mohaisen & Abedulhadi, 2022) ,further studies on the effect of inclined magnetic field just mentioned examined Walter's B fluid as a non-Newtonian fluid and they wear proceed by employing No slip conditions, however in real processes there is constantly a assured degree on slip. Peristalsis reactivity with an effect of inclined magnetic field has received lots of interest, think over the significance of effects of inclined magnetic field in Walter's B fluid (Ali et al., 2016; Jaafar et al., 2024; Khan et al., 2021; Munirathinam et al., 2018; Seth et al., 2018). At present, researchers tend to investigate the action of the inclined magnetic field for peristalsis transport on Non-Newtonian fluids due to the phenomena of conviction, in other words, the dual diffusion of both heat and concentration. We note many of these studies in the references(Alshareef, 2020; DUONG, 2023; Ibraheem & Hummady, 2023; Nadeem & Maraj, 2013; ÖZBAĞ, 2022). Based on the existing literature, the target of the presented research is to examine Numerical computation for the effect of inclined magnetic field on hyperbolic tangent peristalsis flow



suspension in a porous medium. The mathematical formula was created and the constitutive equations were discussed at the small Reynolds number with long wavelength assumptions in section 2, and integrated study of the model was presented in section 3. In section 4, we completed the study by discussing the computational results and graphs.

2. Mathematical Model

Our study intent at a Non-Newtonian hyperbolic tangent fluid with electrical conductivity and incompressibility in an asymmetric duct with a porous medium and walls with the sine waves of width $d_1 + d_2$. In a two-dimensional Cartesian Coordinate system where the influx along *axis X and axis Y* is perpendicular to it and the fluid flows in an inclined magnetic field B_0 . Here we will neglect the effect of both the induced electric and magnetic fields. According to figure 1, the propagation wave speed constant of the wave C straight the walls of this curved channel is written in the following formula:

$$y = \bar{H}_1(\bar{X}, \bar{t}) = d_1 + a_1 \sin\left(\frac{2\pi}{\lambda} (\bar{X} - c\bar{t})\right) \quad (1)$$

$$y = \bar{H}_2(\bar{X}, \bar{t}) = -d_2 - a_2 \sin\left(\frac{2\pi}{\lambda} (\bar{X} - c\bar{t}) + \phi\right)$$

In which $a_1, a_2, d_1, d_2, \lambda, c, t, \phi$ are presented the amplitudes of the wave, breadth of the channel, the wavelength, the wave speed, the time and the phase difference in the range ($0 \leq \phi \leq \pi$), moreover a_1, a_2, d_1, d_2 and ϕ satisfies the frame.

$$a_1^2 + a_2^2 + 2a_1a_2 \cos \phi \leq (d_1 + d_2)^2 \quad (2)$$

The controlling equalization for hyperbolic tangent fluid is formulated as follows (Jaafar et al., 2023) .

$$\bar{t} = -[\bar{S} \tanh(\Gamma \dot{Y})^n] \dot{Y} \quad (3)$$

$$\bar{S} = \mathcal{M}_\infty + (\mathcal{M}_0 + \mathcal{M}_\infty) \quad (4)$$

Where $\mathcal{M}_\infty, \mathcal{M}_0, \Gamma$ and \dot{Y} are presented, Zeroth shear rate viscosity, power law index, and time constant respectively thus \dot{Y} is defined as :

$$\dot{Y} = \sqrt{\frac{1}{2} \sum_i \sum_\eta \dot{Y}_{i\eta} \dot{Y}_{i\eta}} = \sqrt{\frac{1}{2} \pi} \quad (5)$$



Where π is the second invariant strain tensor. We consider the controlling equation (3), for the situation in which \mathcal{M}_∞ equals to zero and $\Gamma\dot{Y}$ less than one. The component of extra stress tensor, it can be formulated as follows:

$$\bar{\tau} = -[\mathcal{M}_\infty (\Gamma\dot{Y})^n] \dot{Y}$$

$$\bar{\tau} = -\mathcal{M}_\infty [1 + n(\Gamma\dot{Y} - 1)] \dot{Y} \quad (6)$$

The equation of continuity, motion, thermal energy and concentration are defined in fixed frame as:

$$\frac{\partial \bar{u}}{\partial \bar{x}} + \frac{\partial \bar{v}}{\partial \bar{y}} = 0 \quad (7)$$

$$p \left(\frac{\partial u}{\partial t} + \bar{u} \frac{\partial \bar{u}}{\partial \bar{x}} + \bar{v} \frac{\partial \bar{u}}{\partial \bar{y}} \right) = -\frac{\partial \bar{p}}{\partial \bar{x}} - \frac{\partial \bar{\tau}_{xx}}{\partial \bar{x}} - \frac{\partial \bar{\tau}_{xy}}{\partial \bar{y}} - \sigma B_\infty^2 \cos B^{**} (\bar{u} \cos B^{**} - \bar{v} \sin B^{**}) - \mathcal{M}_\infty \frac{\bar{u}}{k_\infty} \quad (8)$$

$$p \left(\frac{\partial \bar{v}}{\partial t} + \bar{u} \frac{\partial \bar{v}}{\partial \bar{x}} + \bar{v} \frac{\partial \bar{v}}{\partial \bar{y}} \right) = -\frac{\partial \bar{p}}{\partial \bar{y}} - \frac{\partial \bar{\tau}_{xy}}{\partial \bar{x}} - \frac{\partial \bar{\tau}_{yy}}{\partial \bar{y}} + \sigma B_\infty^2 \sin B^{**} (\bar{u} \cos B^{**} - \bar{v} \sin B^{**}) - \mathcal{M}_\infty \frac{\bar{v}}{k_\infty} \quad (9)$$

$$p c_p \left(\frac{\partial \bar{T}}{\partial t} + \bar{u} \frac{\partial \bar{T}}{\partial \bar{x}} + \bar{v} \frac{\partial \bar{T}}{\partial \bar{y}} \right) = k^* \left(\frac{\partial^2 \bar{T}}{\partial \bar{t}^2} + \frac{\partial^2 \bar{T}}{\partial \bar{x}^2} + \frac{\partial^2 \bar{T}}{\partial \bar{y}^2} \right) + \mathcal{M}_\infty \left(\left(\frac{\partial \bar{u}}{\partial \bar{x}} + \frac{\partial \bar{v}}{\partial \bar{y}} \right)^2 + 2 \left(\frac{\partial^2 \bar{u}}{\partial \bar{x}^2} \right)^2 + 2 \left(\frac{\partial^2 \bar{v}}{\partial \bar{y}^2} \right)^2 \right) \quad (10)$$

$$\frac{\partial \bar{c}}{\partial t} + \bar{u} \frac{\partial \bar{c}}{\partial \bar{x}} + \bar{v} \frac{\partial \bar{c}}{\partial \bar{y}} = D_T \left(\frac{\partial^2 \bar{c}}{\partial \bar{x}^2} + \frac{\partial^2 \bar{c}}{\partial \bar{y}^2} \right) + \frac{D_T k_T}{T_m} \left(\frac{\partial^2 \bar{T}}{\partial \bar{x}^2} + \frac{\partial^2 \bar{T}}{\partial \bar{y}^2} \right) \quad (11)$$

Where \bar{p} , \bar{u} , \bar{v} , \bar{y} , \bar{p} , M_∞ , k_∞ , k^* , B_∞ , σ , D_T , c , k_T , T_m are the fluid density, axial velocity, transverse velocity, transverse coordinate, pressure, viscosity, material constant, permeability parameter, constant inclined magnetic field, electrical conductivity, mass diffusion, mass concentration, thermal diffusion ratio and the mean temperature.

Where

$$\tau_{xx} = -2 M_\infty [1 + n(\Gamma\dot{Y} - 1)] \left(\frac{\partial u}{\partial x} \right)$$

$$\tau_{xy} = -2 M_\infty [1 + n(\Gamma\dot{Y} - 1)] \left(\frac{\partial u}{\partial y} + \frac{\partial v}{\partial x} \right) \quad (12)$$

$$\tau_{yy} = -2 M_\infty [1 + n(\Gamma\dot{Y} - 1)] \left(\frac{\partial v}{\partial y} \right)$$

$$\dot{Y} = \left[2 \left(\frac{\partial u}{\partial x} \right)^2 + \left(\frac{\partial u}{\partial y} + \frac{\partial v}{\partial x} \right)^2 + 2 \left(\frac{\partial v}{\partial y} \right)^2 \right]^{\frac{1}{2}}$$

by using

$$\bar{u} = \frac{\partial \bar{\Psi}}{\partial \bar{y}} \& \bar{v} = -s \frac{\partial \bar{\Psi}}{\partial \bar{x}} \quad (13) \text{ with wave}$$

frame (\bar{x}, \bar{y}) , the motion is steady with these expressions:

$$\bar{X} = \bar{X} - c\bar{t}, \bar{Y} = \bar{y}, \bar{U} = \bar{u} - \bar{c}, \bar{V} = \bar{v}, \bar{P}(\bar{X}, \bar{Y}) = P(\bar{x}, \bar{y}, \bar{t}),$$

$$\bar{T}(\bar{X}, \bar{Y}) = \bar{T}(\bar{x}, \bar{y}, \bar{t}), \bar{C}(\bar{X}, \bar{Y}) = \bar{c}(\bar{x}, \bar{y}, \bar{t}) \quad (14)$$



which are used the dimensionless quantities to find a non- dimensional analysis as below (Hayat, Shafique, et al., 2016) :

$$\chi = \frac{\bar{x}}{\lambda}, y = \frac{\bar{y}}{d_1}, u = \frac{\bar{u}}{c}, V = \frac{\bar{v}}{c}, H_1 = \frac{\bar{H}_1}{d_1}, H_2 = \frac{\bar{H}_2}{d_1}$$

$$P = \frac{\bar{p}d_1^2}{\mathcal{M}_0\lambda c}, D_\sigma = \frac{\bar{k}_0}{d_1^2}, Re = \frac{PCd_1}{\mathcal{M}_0}, S = \frac{d_1}{\lambda},$$

$$Ha = d_1\beta_0 \sqrt{\frac{\sigma}{\mathcal{M}_0}}, \tau = \frac{d_1\bar{\tau}}{\mathcal{M}_0c}, We = \frac{\Gamma c}{d_1}, \beta^{**} = \frac{\bar{\beta}^{**}}{d_1} \quad (15)$$

$$t = \frac{c\bar{t}}{\lambda}, \theta = \frac{\bar{T} - \bar{T}_0}{T_1 - \bar{T}_0}, Ec = \frac{c^2}{Cp(T - T_0)}, Pr = \frac{\mathcal{M}_0Cp}{k^*},$$

$$\Omega = \frac{c-c_0}{c_1-c_0}, Sc = \frac{\mathcal{M}_0}{\rho D_T}, Sr = \frac{\rho k_T D_T (T_1 - \bar{T}_0)}{\mathcal{M}_0 T_m (c_1 - c_0)}$$

Using eqs.(14) , (15) , in eqs. (3) – (12) in wave frame that is taken the following form:

$$S \frac{\partial u}{\partial x} + \frac{\partial v}{\partial y} = 0 \quad (16)$$

$$Re \left(Su \frac{\partial u}{\partial x} + v \frac{\partial u}{\partial y} \right) = -\frac{\partial p}{\partial x} - S \frac{\partial \tau_{xx}}{\partial x} - \frac{\partial \tau_{xy}}{\partial y} - H_a^2 \cos \beta^{**} (u \cos \beta^{**} - V \sin \beta^{**}) - \frac{u}{D_a} \quad (17)$$

$$Re \left(\delta u \frac{\partial v}{\partial x} + v \frac{\partial v}{\partial y} \right) = -\frac{\partial p}{\partial x} - \delta^2 \frac{\partial \tau_{xy}}{\partial x} - \delta \frac{\partial \tau_{yy}}{\partial y} + H_a^2 \delta \sin \beta^{**} (u \cos \beta^{**} - V \sin \beta^{**}) - \delta \frac{v}{D_a} \quad (18)$$

$$Re \left(\psi_y \frac{\partial \theta}{\partial x} + \delta \psi_x \frac{\partial \theta}{\partial y} \right) = -\frac{1}{Pr} \left(\delta^2 \frac{\partial^2 \theta}{\partial x^2} + \frac{\partial^2 \theta}{\partial y^2} \right) + Ec \left[\left(\frac{\partial \psi_y}{\partial y} + \delta^2 \frac{\partial \psi_y}{\partial x} \right)^2 + 2\delta^2 \left(\frac{\partial^2 \psi_y}{\partial x^2} \right)^2 + 2\delta \left(\frac{\partial^2 \psi}{\partial y^2} \right) \right] \quad (19)$$

$$Re \left((\psi_y + 1) \frac{\partial \Omega}{\partial x} + V \frac{\partial \Omega}{\partial y} \right) = \frac{1}{Sc} \left[\delta^2 \frac{\partial^2 \Omega}{\partial x^2} + \frac{\partial^2 \Omega}{\partial y^2} \right] + Sr \left[\delta^2 \frac{\partial^2 \theta}{\partial x^2} + \frac{\partial^2 \theta}{\partial y^2} \right] \quad (20)$$

After a few steps we get :

$$Re \delta \left(\psi_y \frac{\partial \psi_y}{\partial x} - \psi_x \frac{\partial \psi_y}{\partial y} \right) = -\frac{\partial P}{\partial x} - \delta \frac{\partial \tau_{xx}}{\partial x} - \frac{\partial \tau_{xy}}{\partial y} - H_a^2 \cos \beta^{**} \left((\psi_{y+1}) \cos \beta^{xx} + \delta \psi_x \sin \beta^{xx} \right) - \frac{1}{D_a} \psi_y \quad (21)$$

$$Re \delta^3 \left(\psi_y \frac{\partial \psi_y}{\partial x} - \psi_x \frac{\partial \psi_x}{\partial y} \right) = -\frac{\partial P}{\partial y} - \delta^2 \frac{\partial \tau_{xy}}{\partial x} - \delta \frac{\partial \tau_{yy}}{\partial y} + \delta H_a^2 \sin \beta^{xx} \left((\psi_{y+1}) \cos \beta^{xx} + \delta \psi_x \sin \beta^{xx} \right) - \frac{\delta}{D_a} \psi_x \quad (22)$$

$$Re \delta \left(\psi_y \frac{\partial \theta}{\partial x} + \delta \psi_x \frac{\partial \theta}{\partial y} \right) = \frac{1}{Pr} \left(\delta^2 \frac{\partial^2 \theta}{\partial x^2} + \frac{\partial^2 \theta}{\partial y^2} \right) +$$



$$Ec \left[\left(\frac{\partial \psi_y}{\partial y} + \delta^2 \frac{\partial \psi_y}{\partial x} \right)^2 + 2\delta^2 \left(\frac{\partial^2 \psi_y}{\partial x^2} \right)^2 + 2\delta \left(\frac{\partial^2 \psi}{\partial y^2} \right) \right] \quad (23)$$

$$Re \left((\psi_y + 1) \frac{\partial \Omega}{\partial x} - \delta \psi_x \frac{\partial \Omega}{\partial y} \right) = \frac{1}{Sc} \left[\delta^2 \frac{\partial^2 \Omega}{\partial x^2} + \frac{\partial^2 \Omega}{\partial y^2} \right] + Sr \left[\delta^2 \frac{\partial^2 \theta}{\partial x^2} + \frac{\partial^2 \theta}{\partial y^2} \right] \quad (24)$$

And

$$\begin{aligned} \tau_{xx} &= -2 \left(1 + n(w_e \dot{Y} - 1) \right) \left(\frac{\partial^2 \psi}{\partial_x \partial_y} \right), \\ \tau_{xy} &= -2 \left(1 + n(w_e \dot{Y} - 1) \right) \left(\frac{\partial^2 \psi}{\partial y^2} - \delta^2 \frac{\partial \psi}{\partial x} \right), \end{aligned} \quad (25)$$

$$\tau_{yy} = 2S \left(1 + n(w_e \dot{Y} - 1) \right) \left(\frac{\partial^2 \psi}{\partial_x \partial_y} \right),$$

$$\dot{Y} = \left(2\delta^2 \left(\frac{\partial^2 \psi}{\partial_x \partial_y} \right)^2 + \left(\frac{\partial^2 \psi}{\partial y^2} - \delta^2 \frac{\partial \psi}{\partial x} \right)^2 + 2\delta^2 \left(\frac{\partial^2 \psi}{\partial_y \partial_x} \right)^2 \right)^{\frac{1}{2}}$$

where H_a , W_e , R_e and S are the Hartman number, Weissenberg number, Reynolds number and wave number, respectively. Substituting the assumptions of long wavelength in agreement with very small Reynolds number into the equations (21) - (25), we get:

$$\frac{\partial p}{\partial x} = \frac{-\partial \tau_{xy}}{\partial y} - m(\psi_y + 1) \quad (26)$$

$$\text{where } \tau_{xy} = (1 - n) \frac{\partial^2 \psi}{\partial y^2} + nW_e \left(\frac{\partial^2 \psi}{\partial y^2} \right)^2$$

$$m = \frac{1}{n - 1} \sqrt{H_a^2 \cos^2 \beta^{xx} - \frac{1}{D_a}}$$

$$\frac{\partial p}{\partial y} = 0 \quad (27)$$

$$\frac{\partial^2 \theta}{\partial y^2} = -Br \left(\frac{\partial \psi_y}{\partial y} \right)^2 \quad (28)$$

$$\text{where } Br = E_c Pr$$

$$\frac{\partial^2 \Omega}{\partial y^2} = -S_c Sr \frac{\partial^2 \theta}{\partial y^2} \quad (29)$$

Elimination of P between eqs.(21)&(22) yields:

$$\frac{\partial p}{\partial x} = \frac{\partial}{\partial y} \left((1 - n) \frac{\partial^2 \psi}{\partial y^2} + nW_e \left(\frac{\partial^2 \psi}{\partial y^2} \right)^2 \right) - m(\psi_y + 1) \quad (30)$$

We differentiate both sides of equation (30) with respect to y , we have:



$$\frac{\partial^2}{\partial y^2} \left(\frac{\partial^2 \psi}{\partial y^2} + \frac{nW_e}{1-n} \left(\frac{\partial^2 \psi}{\partial y^2} \right)^2 \right) - m \frac{\partial^2 \psi}{\partial y^2} = 0 \quad (31)$$

We mention here the dimensionless boundary conditions that control the flow:

$$\begin{aligned} \psi &= \frac{F}{2} \text{ at } y = h_1 = 1 + a \sin 2\pi x, \\ \psi &= -\frac{F}{2} \text{ at } y = h_2 = -d - b \sin(2\pi x + \phi) \end{aligned} \quad (32)$$

$$\frac{\partial \psi}{\partial y} = -1, \text{ at } y = h_1 \text{ and } y = h_2,$$

$$\theta = 1, \Omega = 1, \text{ at } y = h_1, \theta = 0, \Omega = 0, \text{ at } y = h_2$$

The dimensionless mean flow is defined as (Seth et al., 2018):

$$Q = F + 1 + d, F = \int_{h_2}^{h_1} u dy \quad (33)$$

3. Perturbation Solution

We have a system of non-linear PDEs, eqs.(28),(29),(30) and (31) which is difficult to solve it exactly. Then let use the perturbation method to solve it, for small values of W_e numbe($W_e \ll 1$) and the temperature for small values of Brinkman number ($B_r \ll 1$) as below:

$$\begin{aligned} \psi &= \psi_0 + W_e \psi_1 + O(W_e)^2 \\ \theta &= \theta_0 + W_e \theta_1 + O(W_e)^2 \end{aligned} \quad (34)$$

$$\Omega = \Omega_0 + W_e \Omega_1 + O(W_e)^2$$

Inserting equation (34) into eqs. (28) , (29), (30) and (31) with corresponding boundary conditions (equation (32)) then collecting the coefficients (W_e & B_r) yields the zeroth and the first order systems.

3.1 Zeroth Order System (W_e)

$$\frac{\partial^4 \psi_0}{\partial y^4} - m \frac{\partial^2 \psi_0}{\partial y^2} = 0 \quad (35)$$

$$m = \frac{1}{n-1} \sqrt{H_a^2 \cos^2 \beta^{**} - \frac{1}{D_a}}$$



$$\frac{\partial^2 \theta_0}{\partial y^2} = -B_r \left(\frac{\partial \psi_0}{\partial y} \right)^2 \quad (36)$$

$$\frac{\partial^2 \Omega_0}{\partial y^2} = -S_c S_r \frac{\partial^2 \theta_0}{\partial y^2} \quad (37)$$

$$\psi_0 = \frac{F_0}{2}, \frac{\partial \psi_0}{\partial y} = -1, \theta_0 = 1, \Omega_0 = 1 \text{ at } y = h_1 \quad (38)$$

$$\psi_0 = -\frac{F_0}{2}, \frac{\partial \psi_0}{\partial y} = -1, \theta_0 = 0, \Omega_0 = 0 \text{ at } y = h_2 \quad (39)$$

3.2 Zeroth Order Solution

Solution of equations (35), (36) and (37) are given as:

$$\psi_0 = \frac{e^{-\sqrt{m}y}(e^{2\sqrt{m}y}C_1+C_2)}{m} + C_3 + yC_4 \quad (40)$$

$$C_1 = -\frac{(F_0+h_1-h_2)m}{-2e^{h_1\sqrt{m}}+2e^{h_2\sqrt{m}}+e^{h_1\sqrt{m}}h_1\sqrt{m}+e^{h_2\sqrt{m}}h_1\sqrt{m}-e^{h_1\sqrt{m}}h_2\sqrt{m}-e^{h_2\sqrt{m}}h_2\sqrt{m}}$$

$$C_2 = \frac{e^{h_1\sqrt{m}+h_2\sqrt{m}}(F_0+h_1-h_2)m}{-2e^{h_1\sqrt{m}}+2e^{h_2\sqrt{m}}+e^{h_1\sqrt{m}}h_1\sqrt{m}+e^{h_2\sqrt{m}}h_1\sqrt{m}-e^{h_1\sqrt{m}}h_2\sqrt{m}-e^{h_2\sqrt{m}}h_2\sqrt{m}}$$

$$C_3 = -\frac{(h_1+h_2)(2e^{h_1\sqrt{m}}-2e^{h_2\sqrt{m}}+e^{h_1\sqrt{m}}F_0\sqrt{m}+e^{h_2\sqrt{m}}F_0\sqrt{m})}{2(-2e^{h_1\sqrt{m}}+2e^{h_2\sqrt{m}}+e^{h_1\sqrt{m}}h_1\sqrt{m}+e^{h_2\sqrt{m}}h_1\sqrt{m}-e^{h_1\sqrt{m}}h_2\sqrt{m}-e^{h_2\sqrt{m}}h_2\sqrt{m})}$$

$$C_4 = \frac{2e^{h_1\sqrt{m}}-2e^{h_2\sqrt{m}}+e^{h_1\sqrt{m}}F_0\sqrt{m}+e^{h_2\sqrt{m}}F_0\sqrt{m}}{-2e^{h_1\sqrt{m}}+2e^{h_2\sqrt{m}}+e^{h_1\sqrt{m}}h_1\sqrt{m}+e^{h_2\sqrt{m}}h_1\sqrt{m}-e^{h_1\sqrt{m}}h_2\sqrt{m}-e^{h_2\sqrt{m}}h_2\sqrt{m}}$$

$$m = \frac{1}{n-1} * \sqrt{(Ha)^2 * (\text{Cos}[\beta])^2 - \frac{1}{Da}} \quad (41)$$

3.3 First Order System (W)

$$\frac{\partial^4 \psi_1}{\partial y^4} + \left(\frac{n}{1-n} \right) \frac{\partial^2}{\partial y^2} \left(\left(\frac{\partial^2 \psi_0}{\partial y^2} \right)^2 \right) - m \frac{\partial^2 \psi_1}{\partial y^2} = 0 \quad (42)$$

$$\frac{\partial^2 \theta_1}{\partial y^2} = -2 B_r \left(\frac{\partial \psi_0}{\partial y} \right) \left(\frac{\partial \psi_1}{\partial y} \right) \quad (43)$$

$$\frac{\partial^2 \Omega_1}{\partial y^2} = -S_c S_r \frac{\partial^2 \theta_1}{\partial y^2} \quad (44)$$

$$\psi_1 = \frac{F_1}{2}, \frac{\partial \psi_1}{\partial y} = -1, \theta_1 = 1, \Omega_1 = 1 \text{ at } y = h_1 \quad (45)$$



$$\psi_1 = -\frac{F_1}{2}, \frac{\partial \psi_1}{\partial y} = -1, \theta_1 = 0, \Omega_1 = 0 \text{ at } y = h_2 \quad (46)$$

3.5 The Solution of the Energy Equation

$$\begin{aligned} \theta = & C11 + yC22 + \frac{1}{9(-1+n)^2} ((9C1C2 - 18C1C2n + 9C1C2n^2 + 9A2C1we + \\ & 9A1C2we - 18A2C1nwe - 18A1C2nwe + 9A2C1n^2we + 9A1C2n^2we + \\ & 9A1A2we^2 - 18A1A2nwe^2 + 9A1A2n^2we^2 + \\ & 16C1^2C2^2n^2we^2)(9C2^2e^{2^{3/4}y} \sqrt{\frac{-2+DaHa^2+DaHa^2\cos[2\beta]}{Da}})^{-1+n} EcPr + \\ & 18C1C2e^{2^{2^{3/4}y} \sqrt{\frac{-2+DaHa^2+DaHa^2\cos[2\beta]}{Da}}} EcPr + 9C1^2e^{3^{2^{3/4}y} \sqrt{\frac{-2+DaHa^2+DaHa^2\cos[2\beta]}{Da}}} EcPr \end{aligned} \quad (47)$$

3.6 The Solution of the Concentration Equation

$$\begin{aligned} \Omega = & A11 + yA22 + \frac{1}{9(-1+n)^2} ((9C1C2 - 18C1C2n + 9C1C2n^2 + 9A2C1we + 9A1C2we - \\ & 18A2C1nwe - 18A1C2nwe + 9A2C1n^2we + 9A1C2n^2we + 9A1A2we^2 - 18A1A2nwe^2 + \\ & 9A1A2n^2we^2) \end{aligned} \quad (48)$$

4. Discussion with Numerical Results

In order to better analyze this issue, we will supply a graphical evaluation of the results we acquired in the exact solution section. This section includes two-dimensional diagrams of the solutions for velocity and temperature distribution, in addition to the pressure gradient. It is clear from figures (1-7) of the velocity profile that the flux behavior in this channel is axial flow. In addition, the ultimate value of the velocity profile is noticed in the core of the channel and progressively reductions towards the walls of the channel. Figure (1) presents the behavior of the velocity when the parameter (n) increases, as the velocity is decreasing function in the center of the channel and its left wall while increasing in its right wall. In Figure (2), as the parameter (Ha) increases, we notice that the velocity decreases at the center, while it gains a ultimate value at the channel walls. Figure (3) shows the graphical result of the velocity for characteristic values of the dimensionless parameter (a), as the flow decrease occurs in the center of the channel and its left wall. By increasing this parameter, an opposite behavior is observed



towards the right wall of the channel. Also the effect of parameter (d^*) in figure (4), is due to its apposite behavior to the velocity in the center of the channel and near the right wall, since the velocity decreases in the center and eventually earns its ultimate value, but at the same time it increases near the right wall of this channel. Figure (5) depicts the impact of parameter (b) on the velocity profile, where it reaches a maximum at the left wall of the channel and a minimum at the center of the channel and its right wall. Figure (6) reveals the behavior of parameter (ϕ) , in which the maximum velocity is at the center and the right wall of the channel and it gradually decreases and becomes zero at the left wall of the channel. Figure (7) clearly display the action of parameter (W_e) where the velocity increases the middle of the canal and gradually reductions at the boundary walls. In Figures (8-19) it is illustrating the variation in temperature distribution with different parameters with reference to the Law number (n). Eckert number (Ec), Prandtl number, (Ha), (β) , Darcy number (D_a) , Implitude wave number (a) width number (d), phase difference parameters (ϕ) , and weissberng number (W_e) from figures (8), (14), (15) and (16), the increasing of the values of $(n), (a), (d^*), (b)$ with decreasing it is balance at the center of channel but, for incensing of canal width in two sides, the temperature continuous to rise at near the walls boundary. While the temperature a slight drop in the center but, continuity increaser when its value is decreasing, see Figures (9), (10), (11), (12), (13), (17) and (19). The width number (d) does not affect by change of valve but, a slight drop in the center of channel in each it is explain in figure (18). Figures (20 - 33) represent the Variance of concentration (Ω) across the canal for dissimilarity values of the parameters, $(n, E_c, P_r, S_c, S_r, D_a, \beta, H_a, W_e, a, \delta^*, b, \phi \text{ and } d)$. It can be observed that for all the figures (22, 23, 24, 25, 26, 27 and 33), the concentration (Ω) near canal do nearly concurrent follow the wall waves, what are major arisen by the center for the an asymmetric channel, when the parameters $(E_c, P_r, S_c, S_r, D_a, \beta, H_a \text{ and } W_e)$ More precisely, the decrease



accuse strikingly at the walls of the canal, the concentrations (Ω) increase at the boundary of the Channel walls. Figure (20) explain that an increase in Low number (n), the concentration increasing. The parameters (a, δ^*, b, ϕ and d) does not influence by change of values but, a slight drop in the Center of channel in each change, it is explain in figures (28, 29, 30, 31 and 32).

Velocity Figures

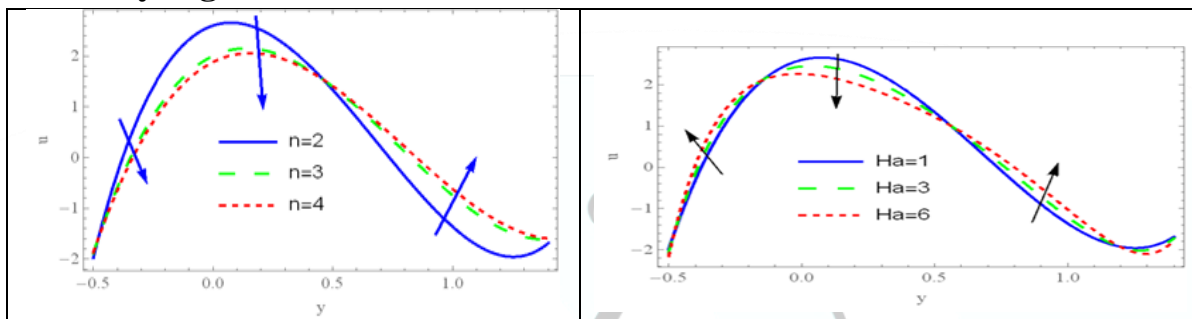


FIGURE1. Behavior of the law number (n) in a wave frame of the sketch of axial velocity distribution ($Ha=1, \beta=\pi/6, Da=2, a=0.5, d^*=0.08, b=0.4, \Phi=\pi/6, F0=0.3, F1=1, d=1, W_e=0.6, x=1$)

FIGURE2. Behavior of the Hartman number (Ha) in a wave frame of the sketch of axial velocity distribution ($n=2, \beta=\pi/6, Da=2, a=0.5, d^*=0.08, b=0.4, \Phi=\pi/6, F0=0.3, F1=1, d=1, W_e=0.6, x=1$)

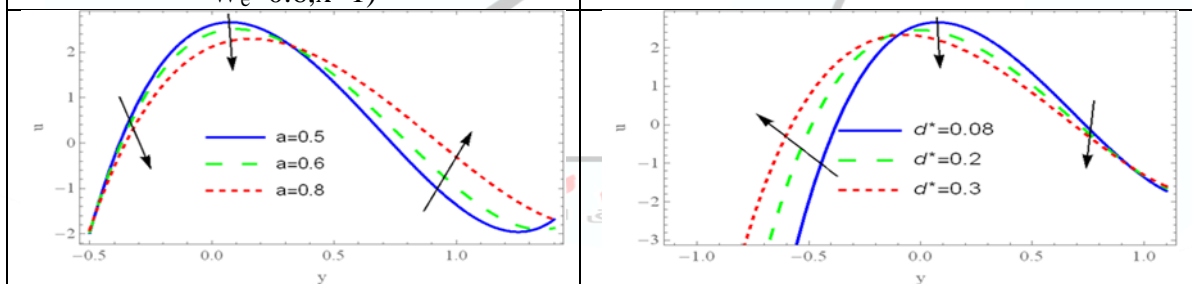


FIGURE3. Behavior of the implitude wave of upper wall (a) in a wave frame of the sketch of axial velocity distribution ($n=2, Ha=1, \beta=\pi/6, Da=2, d^*=0.08, b=0.4, \Phi=\pi/6, F0=0.3, F1=1, d=1, W_e=0.6, x=1$)

FIGURE4. Behavior of the width number (d^*) in a wave frame of the sketch of axial velocity distribution ($n=2, Ha=1, \beta=\pi/6, Da=2, a=0.5, b=0.4, \Phi=\pi/6, F0=0.3, F1=1, d=1, W_e=0.6, x=1$)

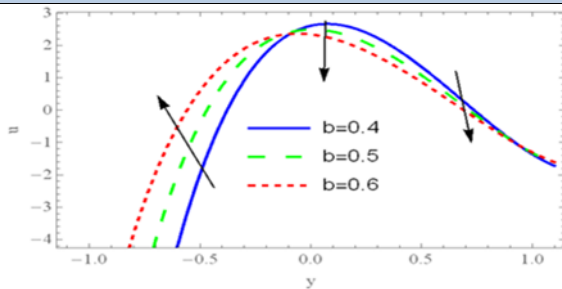


FIGURE5 Behavior of the implitude wave of lower number (b) in a wave frame of the sketch of axial velocity distribution ($n=2$, $Ha=1, \beta=\pi/6, Da=2, a=0.5, d^*=0.08, \Phi=\pi/6, F_0=0.3, F_1=1, d=1, W_e=0.6, x=1$)

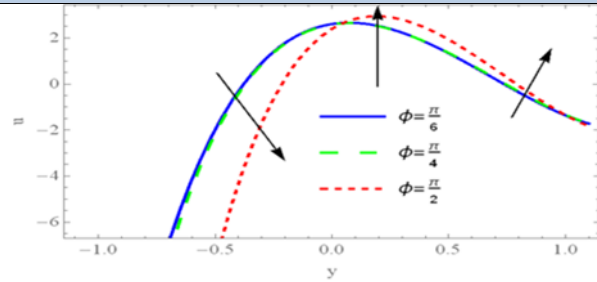


FIGURE6. Behavior of the phase difference (ϕ) in a wave frame of the sketch of axial velocity distribution ($n=2$, $Ha=1, \beta=\pi/6, Da=2, a=0.5, d^*=0.08, b=0.4, F_0=0.3, F_1=1, d=1, W_e=0.6, x=1$)

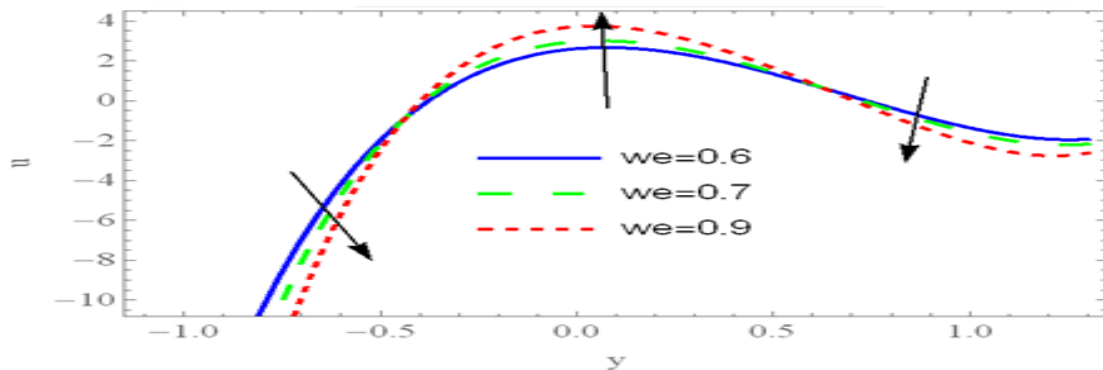


FIGURE7. Behavior of the Weisberg number (b) in a wave frame of the sketch of axial velocity distribution ($n=2, Ha=1, \beta=\pi/6, Da=2, a=0.5, d^*=0.08, b=0.4, \Phi=\pi/6, F_0=0.3, F_1=1, d=1, x=1$)



Temperature Figures

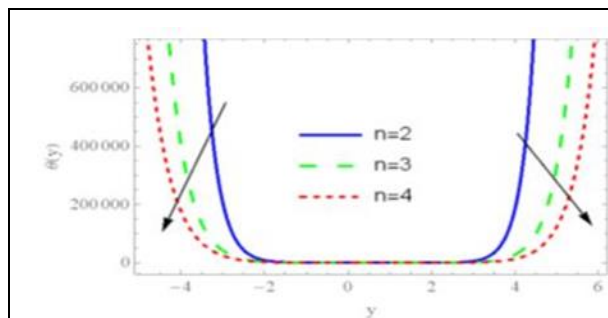


FIGURE8. Behavior of the law number (n) in a wave frame of the sketch of temperature distribution ($Ec=1, Pr=1, Ha=1, \beta=\pi/6, Da=2, a=0.5, d^*=0.08, b=0.4, \Phi=\pi/6, F0=0.3, F1=1, d=1, We_e=0.6, x=1$)

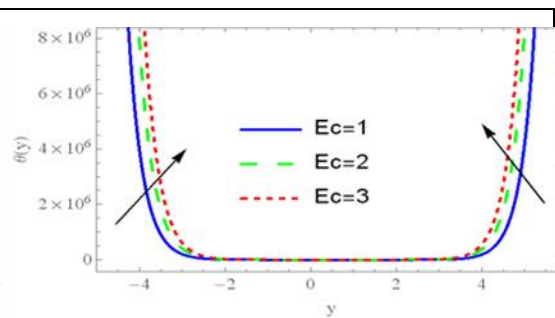


FIGURE9. Behavior of the Eckert number (E_c) in a wave frame of the sketch of temperature distribution ($n=2, Pr=1, Ha=1, \beta=\pi/6, Da=2, a=0.5, d^*=0.08, b=0.4, \Phi=\pi/6, F0=0.3, F1=1, d=1, We_e=0.6, x=1$)

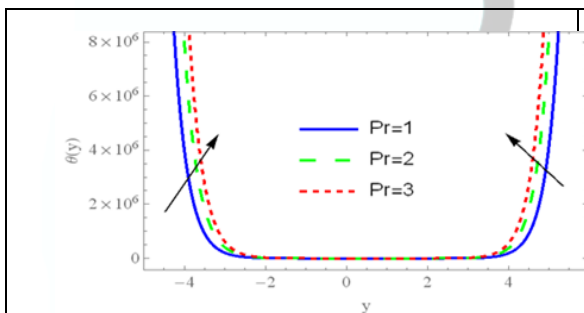


FIGURE10. Behavior of the Prandtl number (Pr) in a wave frame of the sketch of temperature distribution ($n=2, Ec=1, Ha=1, \beta=\pi/6, Da=2, a=0.5, d^*=0.08, b=0.4, \Phi=\pi/6, F0=0.3, F1=1, d=1, We_e=0.6, x=1$)

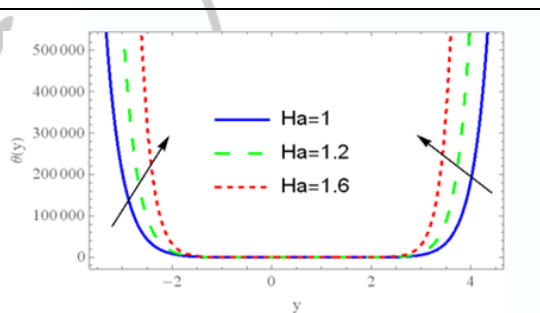


FIGURE11. Behavior of the Hartman number (Ha) in a wave frame of the sketch of temperature distribution ($n=2, Ec=1, Pr=1, \beta=\pi/6, Da=2, a=0.5, d^*=0.08, b=0.4, \Phi=\pi/6, F0=0.3, F1=1, d=1, We_e=0.6, x=1$)

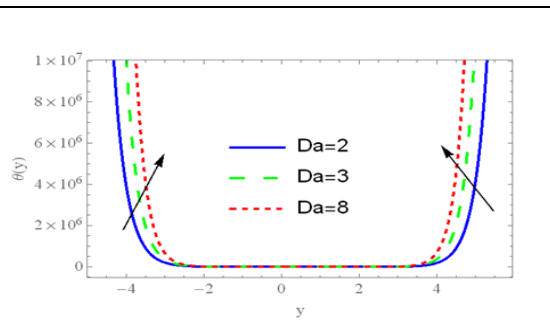
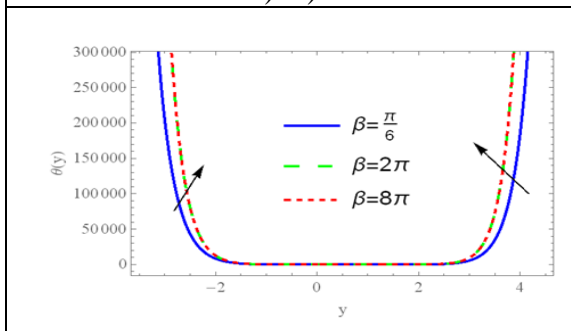




FIGURE12. Behavior of the angle of magnetic field (β) in a wave frame of the sketch of temperature distribution ($n=2$, $Ec=1$, $Pr=1$, $Ha=1$, $Da=2$, $a=0.5$, $d^*=0.08$, $b=0.4$, $\Phi = \pi/6$, $F0=0.3$, $F1=1$, $d=1$, $W_e=0.6$, $x=1$)

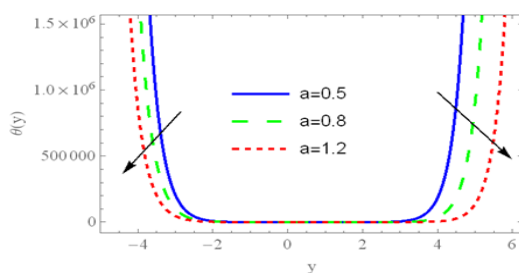


FIGURE13. Behavior of the Darcy number (D_a) in a wave frame of the sketch of temperature distribution ($n=2$, $Ec=1$, $Pr=1$, $Ha=1$, $\beta=\pi/6$, $a=0.5$, $d^*=0.08$, $b=0.4$, $\Phi = \pi/6$, $F0=0.3$, $F1=1$, $d=1$, $W_e=0.6$, $x=1$)

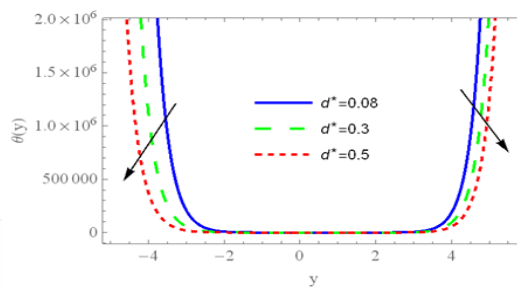


FIGURE14. Behavior of the implitude wave of upper wall (a) in a wave frame of the sketch of temperature distribution ($n=2$, $Ec=1$, $Pr=1$, $Ha=1$, $\beta=\pi/6$, $Da=2$, $d^*=0.08$, $b=0.4$, $\Phi = \pi/6$, $F0=0.3$, $F1=1$, $d=1$, $W_e=0.6$, $x=1$)

FIGURE15. Behavior of the width number (d^*) in a wave frame of the sketch of temperature distribution ($n=2$, $Ec=1$, $Pr=1$, $Ha=1$, $\beta=\pi/6$, $Da=2$, $a=0.5$, $b=0.4$, $\Phi = \pi/6$, $F0=0.3$, $F1=1$, $d=1$, $W_e=0.6$, $x=1$)

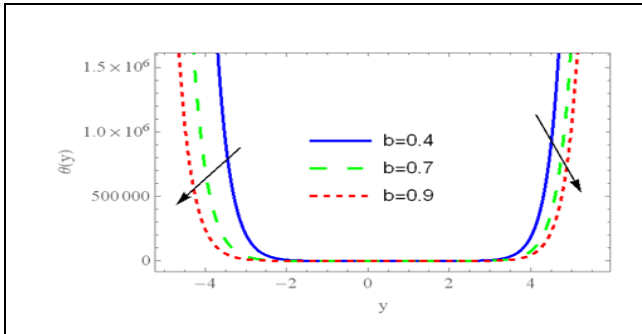


FIGURE16. Behavior of the implitude wave of lower number (b) in a wave frame of the sketch of temperature distribution ($n=2, Ec=1, Pr=1, Ha=1, \beta=\pi/6, Da=2, a=0.5, d^*=0.08, \Phi=\pi/6, F0=0.3, F1=1, d=1, W_e=0.6, x=1$)

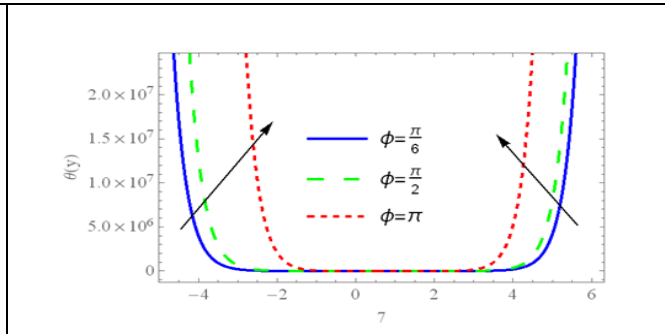


FIGURE17. Behavior of the phase difference (ϕ) in a wave frame of the sketch of temperature distribution ($n=2, Ec=1, Pr=1, Ha=1, \beta=\pi/6, Da=2, a=0.5, d^*=0.08, b=0.4, F0=0.3, F1=1, d=1, W_e=0.6, x=1$)

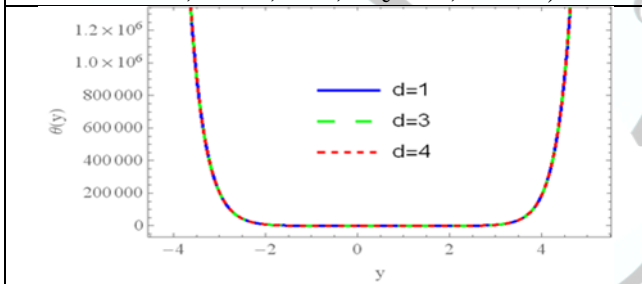


FIGURE18. Behavior of the width number (d) in a wave frame of the sketch of temperature distribution ($n=2, Ec=1, Pr=1, Ha=1, \beta=\pi/6, Da=2, a=0.5, d^*=0.08, b=0.4, \Phi=\pi/6, F0=0.3, F1=1, W_e=0.6, x=1$)

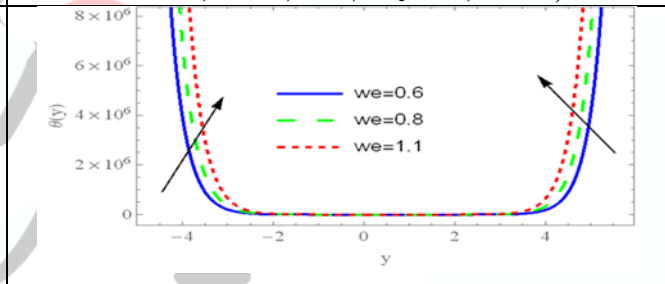
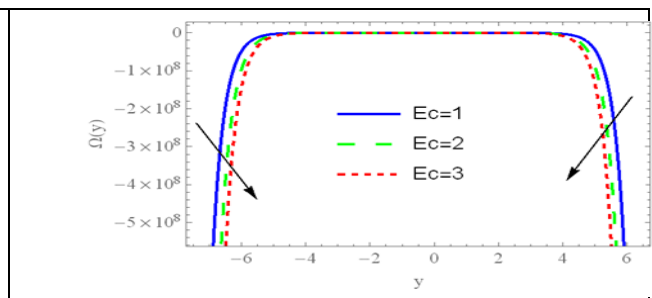
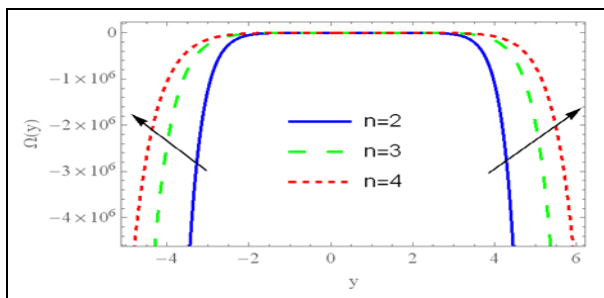


FIGURE19. Behavior of the weissberg number (W_e) in a wave frame of the sketch of temperature distribution ($n=2, Ec=1, Pr=1, Ha=1, \beta=\pi/6, Da=2, a=0.5, d^*=0.08, b=0.4, \Phi=\pi/6, F0=0.3, F1=1, d=1, x=1$)

Concentration Figures





<p>FIGURE20. Behavior of the law number (n) and for all fixed values of parameters ($Ec=1, Pr=1, Sc=2, Sr=3, Ha=1, \beta=\pi/6, Da=2, a=0.5, d^*=0.08, b=0.4, \Phi=\pi/6, F0=0.3, F1=1, d=1, W_e=0.6, x=1$)</p>	<p>FIGURE21. Behavior of the Eckert number (E_c) and for all fixed values of parameters ($n=2, Pr=1, Sc=2, Sr=3, Ha=1, \beta=\pi/6, Da=2, a=0.5, d^*=0.08, b=0.4, \Phi=\pi/6, F0=0.3, F1=1, d=1, W_e=0.6, x=1$)</p>
--	--

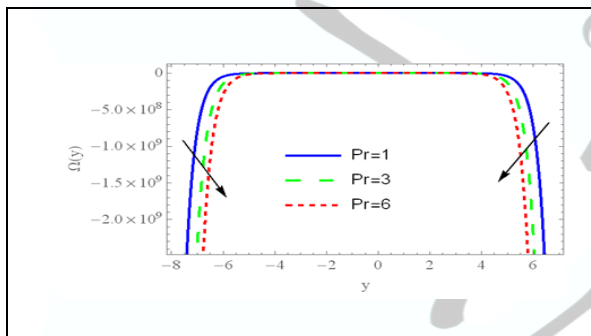


FIGURE22. Behavior of the Prandtl number (P_r) in a wave frame of the sketch of consecration distribution ($n=2, Ec=1, Sc=2, Sr=3, Ha=1, \beta=\pi/6, Da=2, a=0.5, d^*=0.08, b=0.4, \Phi=\pi/6, F0=0.3, F1=1, d=1, W_e=0.6, x=1$)

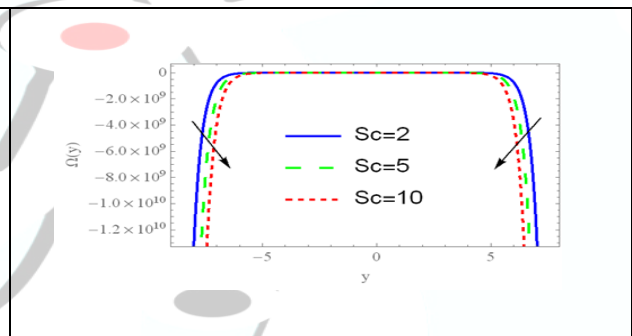


FIGURE23. Behavior of the Schmidt number (S_c) in a wave frame of the sketch of consecration distribution ($n=2, Ec=1, Pr=1, Sr=3, Ha=1, \beta=\pi/6, Da=2, a=0.5, d^*=0.08, b=0.4, \Phi=\pi/6, F0=0.3, F1=1, d=1, W_e=0.6, x=1$)

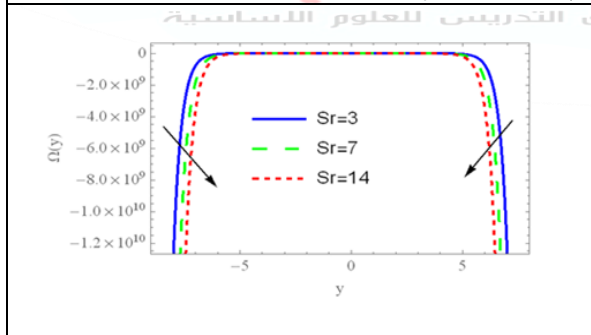


FIGURE24. Behavior of the Soret number (S_r) in a wave frame of the sketch of consecration distribution ($n=2, Ec=1, Pr=1, Sc=2, Ha=1, \beta=\pi/6, Da=2, a=0.5, d^*=0.08, b=0.4,$

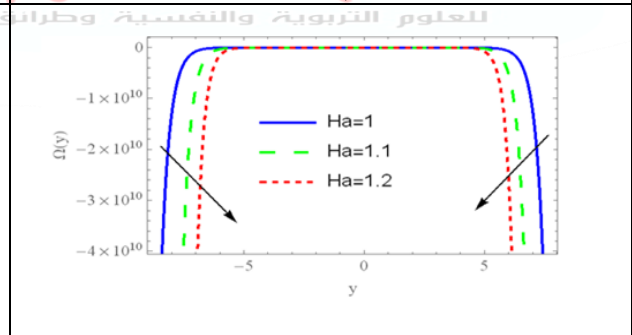
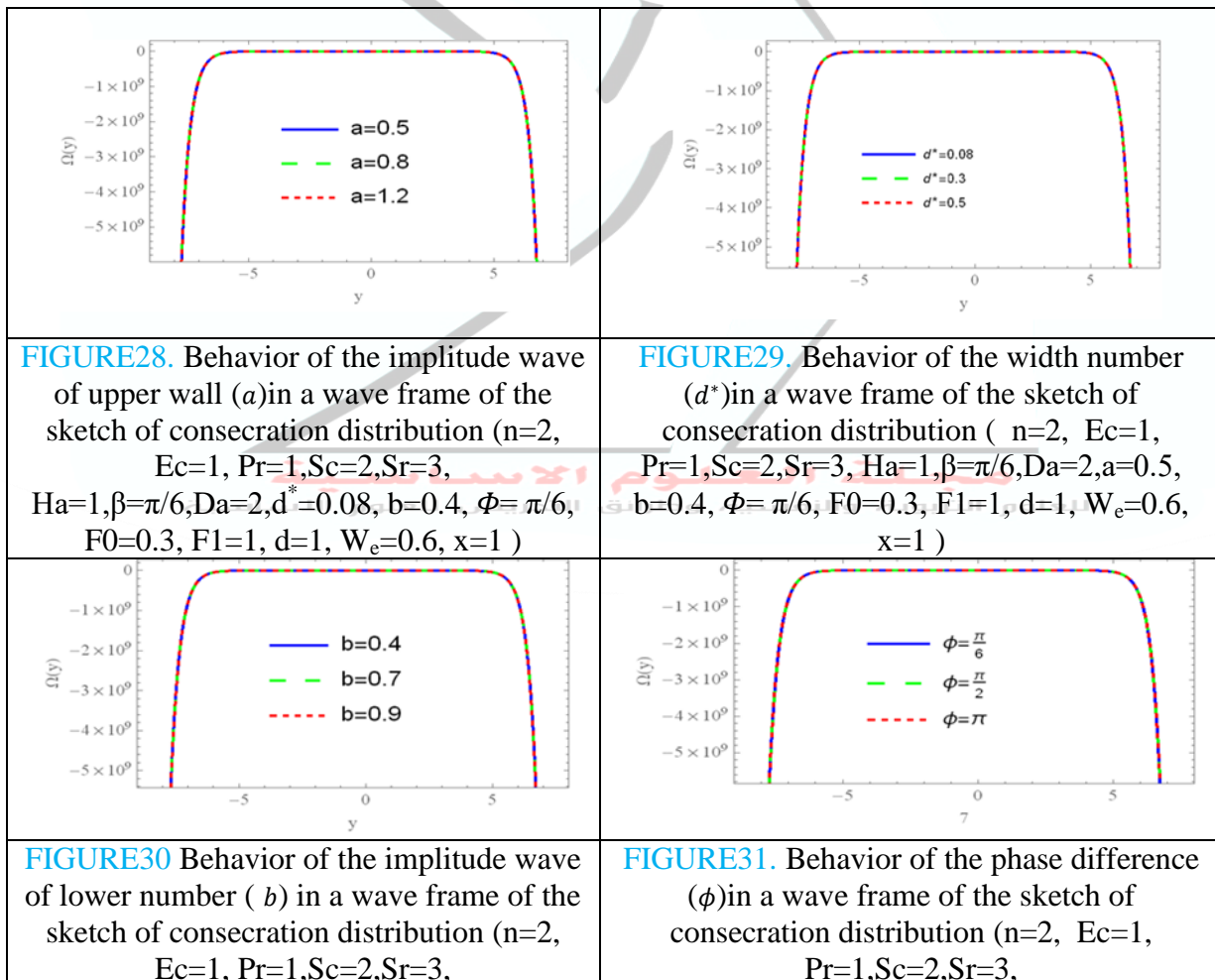
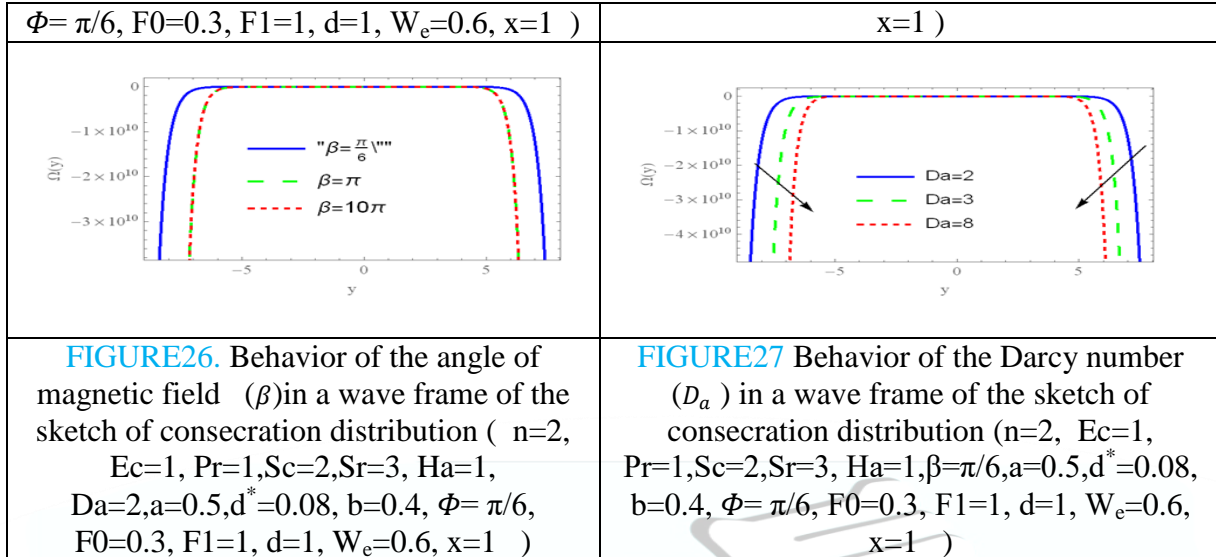


FIGURE25. Behavior of the Hartman number (H_a) in a wave frame of the sketch of consecration distribution ($n=2, Ec=1, Pr=1, Sc=2, Sr=3, \beta=\pi/6, Da=2, a=0.5, d^*=0.08, b=0.4, \Phi=\pi/6, F0=0.3, F1=1, d=1, W_e=0.6,$





$Ha=1, \beta=\pi/6, Da=2, a=0.5, d^*=0.08, \Phi=\pi/6, F0=0.3, F1=1, d=1, W_e=0.6, x=1$	$Ha=1, \beta=\pi/6, Da=2, a=0.5, d^*=0.08, b=0.4, F0=0.3, F1=1, d=1, W_e=0.6, x=1$
<p>FIGURE32. Behavior of the width number (d) in a wave frame of the sketch of consecration distribution ($n=2, Ec=1, Pr=1, Sc=2, Sr=3, Ha=1, \beta=\pi/6, Da=2, a=0.5, d^*=0.08, b=0.4, \Phi=\pi/6, F0=0.3, F1=1, W_e=0.6, x=1$)</p>	<p>FIGURE33. Behavior of the weissberg number (W_e) in a wave frame of the sketch of consecration distribution ($n=2, Ec=1, Pr=1, Sc=2, Sr=3, Ha=1, \beta=\pi/6, Da=2, a=0.5, d^*=0.08, b=0.4, \Phi=\pi/6, F0=0.3, F1=1, d=1, x=1$)</p>

7. Conclusion

According to the nature of the relevant complex constitutive equations showing the impact on the Peristalsis flux of inclined Magnetic field of hyperbolic tangent non-Newtonian fluid in a porous medium and an asymmetric sinusoidal channel, the regular Perturbation method used in this study provided clear success in dealing with such a model of equations, as it gave accurate solutions in peristalsis flux without any conditions imposed on all physical quantities that emerge in the foundational equations. For this study, the axial velocity function, temperature distribution and concentration equation were obtained, in addition to performing a parametric analysis through graphs using the (Mathematica) mathematical program, and the results extracted are the following:

1- When the augmentation in the values of the parameters (ϕ) and (W_e) Leads to an augmentation in the value of the vector velocity the middle of the channel, while an augmentation in the values of the parameters (n, H_a, a) and (d^*), leads to decrease in the value of the velocity, but, when the value of the parameters (D_a, d) and (β) changes, no effect appears on the value of the velocity.



2- In the case of the temperature characteristics function, the increasing values of the parameters (b, a, n) and (d^*) lead to an decrease in the temperature in the core of the canal and its increase at the walls, but the rise in the values of the parameters ($E_c, P_r, H_a, \beta, D_a, \phi$) and (W_e) means increasing in the temperature.

3- The concentration an augmentation in the boundary of the canal walls as augmentation of the parameter(n), while the an augmentation in the value of the parameters ($E_c, P_r, S_c, S_r, H_a, \beta, D_a, w_e$) give rise to decrease in the value of the concentration.

4 - When the value of the parameters (a, b, d^* , Φ , d) changes, no effect appears on the value of the concentration.

Acknowledgement

Acknowledgements and Reference heading should be left justified, bold, with the first letter capitalized but have no numbers. Text below continues as normal.

References

- 1.Ali, F., Saqib, M., Khan, I., & Ahmad Sheikh, N. (2016). Application of Caputo-Fabrizio derivatives to MHD free convection flow of generalized Walters'-B fluid model. *The European Physical Journal Plus*, 131(10), 377.
- 2.Alshareef, T. S. (2020). Impress of rotation and an inclined MHD on waveform motion of the non-Newtonian fluid through porous canal. *Journal of Physics: Conference Series*, 1591(1), 12061.
- 3.DUONG, A. N. H. T. (2023). Liouville-type theorem for one-dimensional porous medium systems with sources. *Turkish Journal of Mathematics*, 47(6), 1733–1745.
- 4.Evans, L. C. (2022). *Partial differential equations* (Vol. 19). American Mathematical Society.
- 5.Hage, A. K., & Hummady, L. Z. (2022). Influence of inclined magnetic field and heat transfer on peristaltic transfer Powell-Eyring fluid in asymmetric channel and porous medium. *International Journal of Nonlinear Analysis and Applications*, 13(2), 631–642.
- 6.Hayat, T., Rafiq, M., & Ahmad, B. (2016). Soret and Dufour effects on MHD peristaltic flow of Jeffrey fluid in a rotating system with porous medium. *PloS One*, 11(1), e0145525.
- 7.Hayat, T., Shafique, M., Tanveer, A., & Alsaedi, A. (2016). Magnetohydrodynamic effects on peristaltic flow of hyperbolic tangent nanofluid with slip conditions and Joule



heating in an inclined channel. *International Journal of Heat and Mass Transfer*, 102, 54–63.

8. Ibraheem, R. G., & Hummady, L. Z. (2023). Effect of Couple-stress with Slip Condition and Rotation on Peristaltic Flow of a Powell-Eyring Fluid with the Influence of an Inclined Asymmetric Channel with Porous Medium. *Journal of Basic Sciences*, 10(17).

9. Jaafar, Z. A., Hummady, L. Z., & Thawi, M. H. (2024). Effects of Rotation and Inclined Magnetic Field on Walters' B Fluid in a Porous Medium using perturbation method or technique. *Iraqi Journal of Science*.

10. Jaafar, Z. A., Thawi, M. H., & Hummady, L. Z. (2023). *Impact of Couple Stress with Rotation on Walters , B Fluid in Porous Medium*. 189–201.

11. Khan, M. I., Khan, S. U., Jameel, M., Chu, Y.-M., Tlili, I., & Kadry, S. (2021). Significance of temperature-dependent viscosity and thermal conductivity of Walter's B nanoliquid when sinusoidal wall and motile microorganisms density are significant. *Surfaces and Interfaces*, 22, 100849.

12. Kumar, S. R. (2016). MHD peristaltic transportation of a conducting blood flow with porous medium through inclined coaxial vertical channel. *International Journal of Bio-Science and Bio-Technology*, 8(1), 11–26.

13. Mekheimer, K. S. (2008). Effect of the induced magnetic field on peristaltic flow of a couple stress fluid. *Physics Letters A*, 372(23), 4271–4278.

14. Mohaisen, H. N., & Abedulhadi, A. M. (2022). Effects of the Rotation on the Mixed Convection Heat Transfer Analysis for the Peristaltic Transport of Viscoplastic Fluid in Asymmetric Channel. *Iraqi Journal of Science*, 1240–1257.

15. Munirathinam, S., Ragavan, C., & Kalaivanan, R. (2018). The impact of aligned magnetic field on Walters Liquid B fluid over a stretching surface with Rosseland diffusion approximation. *Malaya J. Matematik*, 6(3), 658–663.

16. Nadeem, S., Akram, S., & Akbar, N. S. (2013). Simulation of heat and chemical reactions on peristaltic flow of a Williamson fluid in an inclined asymmetric channel. *Iranian Journal of Chemistry and Chemical Engineering (IJCCE)*, 32(2), 93–107.

17. Nadeem, S., & Maraj, E. N. (2013). The mathematical analysis for peristaltic flow of hyperbolic tangent fluid in a curved channel. *Communications in Theoretical Physics*, 59(6), 729.

18. ÖZBAĞ, F. (2022). Numerical simulations of traveling waves in a counterflow filtration combustion model. *Turkish Journal of Mathematics*, 46(4), 1424–1435.

19. Seth, G. S., Mishra, M. K., & Tripathi, R. (2018). MHD free convective heat transfer in a Walter's liquid-B fluid past a convectively heated stretching sheet with partial wall slip. *Journal of the Brazilian Society of Mechanical Sciences and Engineering*, 40, 1–11.

JOBS



مجلة العلوم الأساسية
Journal of Basic Science



Print -ISSN 2306-5249

Online-ISSN 2791-3279

العدد الثاني والعشرون

٢٠٢٤م / ١٤٤٥هـ



مجلة العلوم الأساسية
للعلوم التربوية والنفسية وطرائق التدريس للعلوم الأساسية